Journal of Earth, Environment Science and Agricultural Research

Research Article

Volume 1 | Issue 2

# Optimization and Comparative Analysis of Artificial Lift Systems for Horizontal Well Production: A Case Study of Gas Lift, Beam Lift, and ESP Systems

**Ekrem Alagoz[1*], Mehmet Serif Arslan[2], Muhammed Said Ergul[3], Mouad Al Krmagi[4] and Mubarek Alpkiray[5]**

[1]Turkish Petroleum Corporation (TPAO)
[2]Istanbul Technical University
[3]Izmir Katip Celebi University
[4]Texas A&M University
[5]General Directorate of Mineral Research and Exploration (MTA)

**[*]Corresponding Author:** Ekrem Alagoz, Turkish Petroleum Corporation (TPAO), Engineering Department, Sogutozu Nizami Gencevi Street No:10, 06510 Cankaya, Ankara, Turkey.

**Submitted:** 29 Nov 2024 **Accepted:** 08 Dec 2024 **Published:** 12 Dec 2024

***Citation:*** Alagoz E, Arslan MS, Ergul MS, Krmagi MA, Alpkiray M (2024) Optimization and Comparative Analysis of Artificial Lift Systems for Horizontal Well Production: A Case Study of Gas Lift, Beam Lift, and ESP Systems. CSK J of E, E Science & Agriculture Research. Research Article 1(2): 01-13.

***Abstract***

*This study presents an optimization and comparative analysis of three artificial lift systems—gas lift, beam lift, and electric submersible pump (ESP)—for producing hydrocarbons from a horizontal well. The well, with a true vertical depth (TVD) of 9,000 ft and a measured depth (MD) of 18,000 ft, features challenging reservoir conditions including a gas-liquid ratio (GLR) of 200 Scf/STBL and a bottom-hole temperature of 180°F. To determine the most suitable lifting system, we assess the efficiency and flexibility of each system to sustain production until the well reaches its economic limit of 5 STB/day. The analysis considers oil properties (38° API), water-oil ratio (WOR of 1 BW/BO), and available infrastructure such as a nearby gas pipeline operating at 1014.7 psia. Key changes in each system are evaluated as the well depletes, including modifications to accommodate declining reservoir pressure and production rates. After a detailed comparison, the most effective artificial lift method is selected based on technical performance, operational adaptability, and overall cost efficiency. The findings of this study provide practical recommendations for optimizing artificial lift strategies in horizontal well scenarios.*

**Keywords**: Artificial Lift Systems, Gas Lift, Electric Submersible Pump (ESP), Beam Lift, Horizontal Well Production

## Introduction

Artificial lift systems are crucial in maintaining and enhancing hydrocarbon production from oil and gas wells, particularly as natural reservoir energy depletes over time. As a well progresses beyond its natural flowing life, pressure support mechanisms, such as gas lift, beam lift, and electric submersible pump (ESP) systems, are implemented to sustain production to the economic limit. Each of these artificial lift techniques has its unique advantages and challenges, and the selection of the most appropriate system depends on factors such as reservoir conditions, production rates, well geometry, and operational flexibility.

The focus of this study is a horizontal well with a true vertical depth (TVD) of 9,000 feet and a measured depth (MD) of 18,000 feet. The well produces hydrocarbons with an oil gravity of 38° API and a gas-liquid ratio (GLR) of 200 Scf/STBL. As the reservoir depletes and production rates decline, artificial lift will be required to maintain oil production, particularly as the well approaches the economic limit of 5 STB/day. A nearby gas pipeline operating at 1014.7 psia (60 degF) provides an additional option for using gas lift if needed.

To predict future production and select the optimal artificial lift system, we analyze the well's performance using a decline curve (Figure 1), which shows the well's natural flow over 47 days before requiring artificial lift. Decline curve analysis enables the forecasting of future oil rates and corresponding bottom-hole pressure, which are essential in evaluating the efficiency and flexibility of various artificial lift methods.

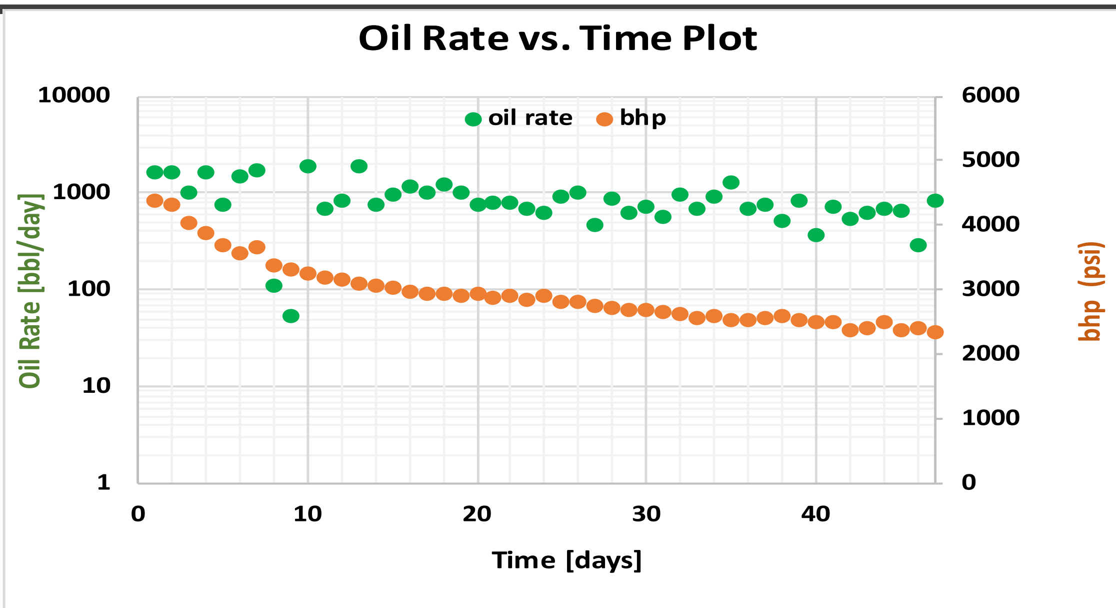


**Figure 1 – Oil Rate vs Time Plot of designated well**

In this study, we will compare the gas lift, beam lift, and ESP systems based on their performance in sustaining production as the well depletes. Special attention will be given to system efficiency, operational adaptability, and changes required over time to keep production above the economic threshold. The goal is to determine the most cost-effective and technically suitable lift system for the long-term operation of the horizontal well under the given conditions (Table 1). It is important to note that the deepest vertical part of the well is at 8,000 TVD. The well transitions to horizontal over the final 1,000 feet of TVD. Finally, the bottom hole pressure numbers exist at the deepest TVD at 9,000 feet.

**Table 1 – Horizontal Well Data**

| | |
|---|---|
| **Depth (TVD), ft** | **9,000** |
| **Measured Depth (MD), ft** | **18,000** |
| **Oil API Gravity** | **38** |
| **Water Specific Gravity** | **1.02** |
| **Gas Specific Gravity** | **0.7** |
| **Gas Liquid Ratio (GLR) (Scf/STBL)** | **200** |
| **WOR ($B_W/B_O$)** | **1** |
| **Separator Pressure, psia** | **65** |
| **Separator Temperature, degF** | **100** |
| **Tubing ODxID, in** | **2.875”x 2.441”** |
| **Casing ID, in** | **7** |
| **Bottom Hole Temperature, degF** | **180** |

## Previous Works

Several studies have provided critical insights into optimizing well production and evaluating the effectiveness of various stimulation and artificial lift techniques, which are essential for enhancing horizontal well performance. Alagoz et al. (2023) conducted an optimization study on fracture treatment design for vertical wells, demonstrating how customized fracture strategies can significantly improve production rates and reduce operational risks [1]. Similarly, Alagoz and Dundar (2023) performed a comparative analysis of production forecasts for fractured versus non-fractured vertical gas wells, offering valuable perspectives on the impact of well stimulation on production efficiency [2]. These studies contribute to the broader understanding of fracture design and well performance, which are crucial for evaluating artificial lift systems in horizontal wells.

In the context of unconventional reservoirs, Laalam et al. (2024) focused on the prediction and forecasting of production from unconventional wells in the Wolfcamp A formation using empirical correlations and time series models. Their findings emphasize the importance of advanced modeling techniques in forecasting production behaviors, which are essential for optimizing artificial lift systems like gas lift and ESP [3]. Further exploration of unconventional reservoir recovery was presented by Dehdouh et al. (2024), who highlighted the potential of fishbone drilling technology in the Bakken Formation. Their research demonstrates innovative approaches for increasing reservoir contact and improving recovery rates, which have direct implications for artificial lift system design in challenging formations [4].

Environmental and operational considerations are also critical when optimizing production systems. Al Krmagi (2024) explored the environmental impacts of hydraulic fracturing and discussed various treatment technologies for managing flowback water. This research provides essential insights into the sustainable management of fracturing fluids, which is vital for minimizing the environmental footprint of artificial lift operations [5]. Moreover, Alagoz and Mengen (2024) used advanced shale characterization techniques to investigate mineralogical and chemical properties that influence reservoir behavior, which is critical for understanding fluid dynamics and optimizing artificial lift system design [6].

Further work by Alagoz and Sharma (2021) investigated shale-fluid interactions and their effect on proppant embedment using NMR techniques, shedding light on how these interactions impact fracture conductivity and well performance [7]. Alpkiray and Dundar (2023) offered a broader perspective on hydraulic fracturing, addressing its benefits, concerns, and future developments, which are crucial for understanding the role of stimulation techniques in optimizing artificial lift systems [8].

Additionally, Alagoz et al. (2022) introduced new experimental methods for studying proppant embedment in shales, directly linking the findings to the efficiency of fracture conductivity maintenance and the design of artificial lift systems [9].

The role of numerical simulation in optimizing production and artificial lift systems has also been a focal point of recent research. Alagoz, Dundar, and Al Krmagi (2024) developed a numerical simulator for production forecasting in multi-lateral oil wells using MATLAB, which demonstrates the potential of simulation tools in enhancing well performance and artificial lift system efficiency [10].

Similarly, Alagoz and Dundar (2024) explored transient flow and pressure dynamics in gas wells, offering valuable insights into pressure drop analysis and its effect on gas lift and other artificial lift systems [11]. Finally, Alagoz, Dundar, and Al Krmagi (2024) expanded their work by simulating a multilateral saturated reservoir, highlighting the complexities of reservoir dynamics and the critical role of simulation in optimizing artificial lift strategies [12].

Collectively, these studies contribute to the understanding and optimization of artificial lift systems, providing a comprehensive basis for the comparative analysis of gas lift, beam lift, and ESP systems in horizontal wells.

## Solution Approach

The decline curve shows the well performance to the end of the natural flowing life of the well (time = 47 days). After this time some form of artificial lift will be needed. Future oil rates and associated bottom hole pressure can be predicted using.

$$q_o = -157.1\ln(t) + 1098$$

$$p_{wf} = 2{,}575 - 2.4(t)$$

$q_o =$ daily oil rate (STBO/day)

$p_{wf} =$ bottom hole pressure (psig)

$t =$ time (days)

Analyzing the production decline curve reveals a rapid drop in bottom hole pressure, from approximately 4500 psi to 2100 psi over a short period. This sharp decline indicates a significant reduction in reservoir pressure, suggesting that the reservoir lacks sufficient natural drive to sustain prolonged production. The steep pressure decline also points to limited permeability, characteristic of an unconventional reservoir. Such reservoirs typically require enhanced recovery methods, such as artificial lift systems, to maintain production rates as natural reservoir energy quickly diminishes. This paper will sequentially design the gas lift, beam lift, and ESP systems.

### 2.1. Gas Lift Design

This paper presents the design of a gas lift (GL) system to optimize oil production for the given well, with an economic flow rate limit set at 5 STB/day. Using model equations, the time at which the reservoir becomes economically unviable will be calculated. This analysis aims to assess the performance of the gas lift system and determine when further interventions or adjustments may be necessary to sustain profitability.

$$q_o = -157.1\ln(t) + 1098 = 5\ stbpd, then\ t = 1051\ days.$$

Additionally, this paper will calculate the bottom hole pressure at the point beyond which the reservoir becomes economically unprofitable. This calculation will provide insights into the critical pressure threshold that must be maintained to ensure continued profitability in oil production.

$$pwf = 2575 - 2.4(1051) = 52.6\ psi$$

At the end of the analysis, the bottom hole pressure is approximately 53 psi, indicating that the reservoir can achieve the economic flow rate limit of 5 STB/day. The next step involves optimizing the gas-liquid ratio (GLR) design for this well. To proceed, the average density will first be calculated using the Utilities package in the Excel file.

Given a water-oil ratio (WOR) of 1 BW/BO, this indicates a water cut of 50 percent. The specific gravity of the oil can be calculated using the following equation:

38 API= 141.5/SG-131.5 = SG of oil (ɣoil) = 0.8348

Average specific gravity of the mixture,
ɣmix = (0.8348+1.02)/2 = 0.9274

The problem statement indicates the availability of a pipeline capable of supplying sufficient gas for the gas lift (GL) operation, allowing for the option to back pressurize this gas into the pipeline. Consequently, the necessary surface facilities are in place for the operation.

Initially, the design will commence with a gas-liquid ratio (GLR) of 1000 Scf/STB. If the continuous gas lift system fails, additional gas will need to be introduced to sustain production levels. Utilizing the Utilities package in the Excel file, a table will be constructed to facilitate the analysis of these parameters.

**Table 2 – Gas Lift Program**

| t (days) | Qo(model) | Pwf(model) | GLR | Pwf(calculated) | comment |
|---|---|---|---|---|---|
| 47 | 493,5268265 | 2462,2 | 1000 | 1064 | GL is working |
| 100 | 374,9882808 | 2335 | 1000 | 938 | GL is working |
| 150 | 311,3302588 | 2215 | 1000 | 872 | GL is working |
| 200 | 266,1641735 | 2095 | 1000 | 827 | GL is working |
| 250 | 231,1306359 | 1975 | 1000 | 793 | GL is working |
| 300 | 202,5061515 | 1855 | 1000 | 765 | GL is working |
| 350 | 178,3044947 | 1735 | 1000 | 742 | GL is working |
| 400 | 157,3400661 | 1615 | 1000 | 722 | GL is working |
| 450 | 138,8481295 | 1495 | 1000 | 705 | GL is working |
| 500 | 122,3065285 | 1375 | 1000 | 688 | GL is working |
| 550 | 107,3428303 | 1255 | 1000 | 673 | GL is working |
| 600 | 93,68204413 | 1135 | 1000 | 659 | GL is working |
| 650 | 81,11533903 | 1015 | 1000 | 646 | GL is working |
| 700 | 69,4803874 | 895 | 1000 | 634 | GL is working |
| 750 | 58,64850657 | 775 | 1000 | 621 | GL is working |
| 800 | 48,51595876 | 655 | 1000 | 609 | GL is working |
| 805 | 47,53776245 | 643 | 1000 | 608 | GL is working |
| 810 | 46,56562312 | 631 | 1000 | 606 | GL is working |
| 815 | 45,59946622 | 619 | 1000 | 605 | GL is working |
| 820 | 44,63921858 | 607 | 1000 | 604 | GL is working |
| 825 | 43,68480835 | 595 | 1000 | 603 | MORE GAS NEEDED |
| 830 | 42,73616498 | 583 | 2000 | 548 | GL is working |
| 835 | 41,7932192 | 571 | 2000 | 547 | GL is working |
| 840 | 40,85590298 | 559 | 2000 | 546 | GL is working |
| 850 | 38,99789313 | 535 | 2000 | 544 | MORE GAS NEEDED |
| 860 | 37,16161489 | 511 | 5000 | 511 | MORE GAS NEEDED |
| 870 | 35,34656577 | 487 | 10000 | 501 | MORE GAS NEEDED |
| 880 | 33,55226053 | 463 | 15000 | 506 | MORE GAS NEEDED |

After 825 days, the initial gas-liquid ratio (GLR) of 1000 Scf/STB is no longer effective, necessitating an increase in the gas supply to sustain production. By doubling the amount of gas introduced into the well, production is extended for an additional 25 days. However, at this stage, further increases in gas injection may lead to excessive friction within the system. Continuing to add gas in an attempt to extend production to 1051 days results in a significantly high demand for gas, highlighting the challenges associated with maintaining optimal production levels under these conditions.

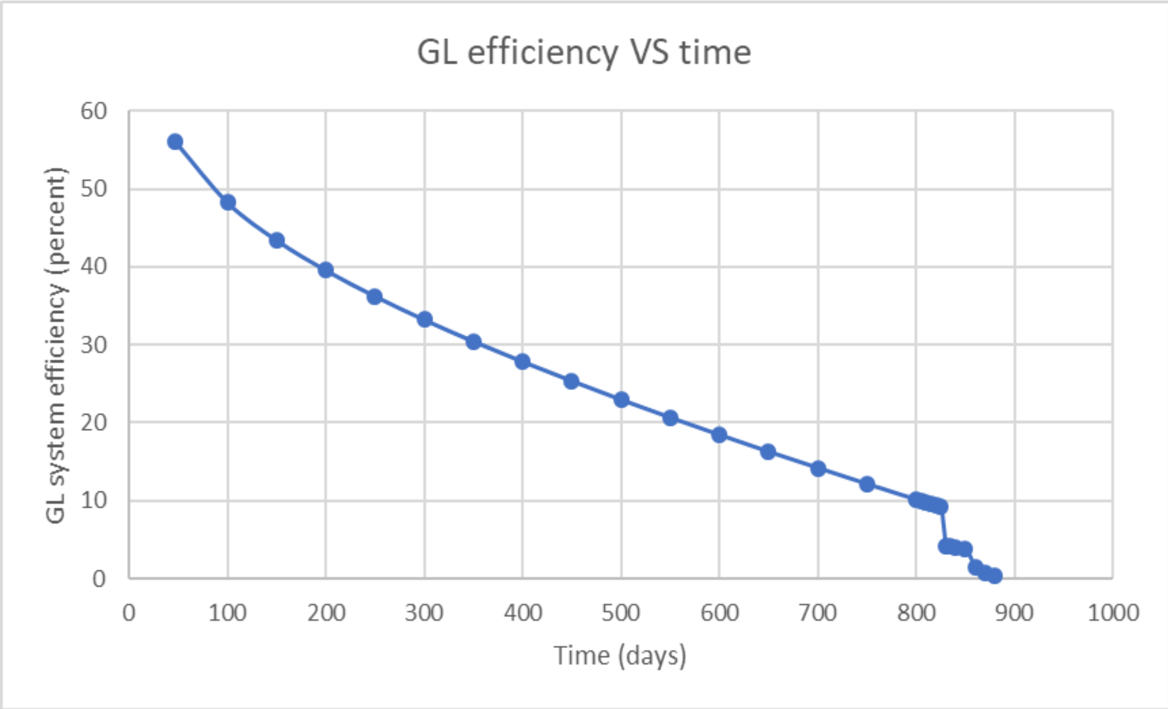


**Figure 2 – GL system efficiency chart**

Above graph and figure is built by using following equations.

$$e_{GL} = \frac{HHP_{out}}{BHP_{in}}$$

$e_{GL}$ = Gas lift system efficiency (fraction)

$HHP_{out}$ = hydraulic horsepower out (hp)

$BHP_{in}$ = break or brake horsepower in (hp)

$$HHP_{out} = 1.7x10^{-5} qp_{wf}$$

$q$ = reservoir liquid rate (STBL/day)

$p_{wf}$ = pressure left from the reservoir at the point of gas injection (psia)

$BHP_{in}$ = compressor power (BHP)

$$HP \cong 2.23x10^{-4} q\left[\left(\frac{p_{discharge}}{p_{suction}}\right)^{0.2} - 1\right]$$

$q$ = gas rate (Scf/Day)

both pressures are in psi

$HP$ = compressor horsepower

## 2.2. Beam Lift Design

For the beam lift design, the QROD program is employed to calculate various parameters. Additionally, rod design is performed manually and subsequently verified using an Excel spreadsheet. The pump position is optimized by selecting Point A, as depicted in Figure 3, ensuring safe operation and longevity of the pump.

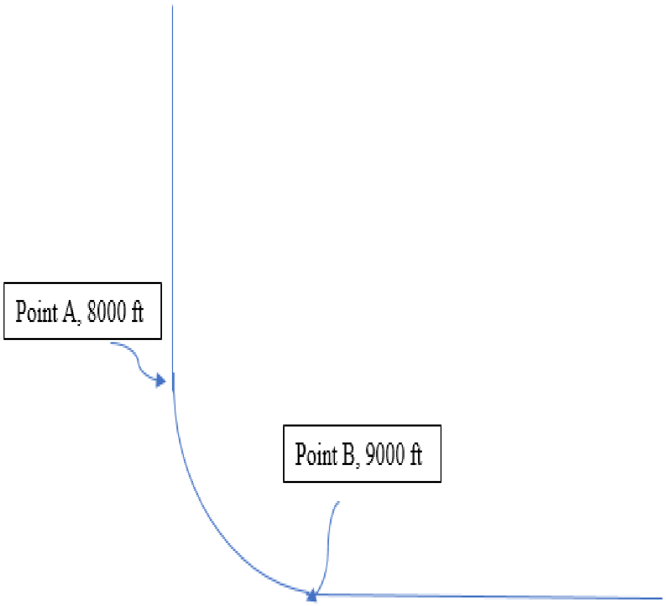


**Figure 3 – Well schematic of beam lift design**

To facilitate the operation of this design, the reservoir oil must overcome the curved section of the well. In the calculations, a pump intake pressure of 50 psi is utilized. The pressure at Point B can then be calculated as follows:

P = 1000 ft * 0.433 psi/ft * 0.9274 + 50 psi = 452 psi

This indicates that a pressure of 452 psi is required at Point B to elevate the liquid to Point A, allowing the beam lift pump to transport it to the surface. Assuming that frictional pressure drop in the horizontal section of the well is negligible, a minimum pressure of 452 psi is necessary for liquid production in this well. As illustrated in Figures 4 and 5, the majority of the production occurs at pressures exceeding 452 psi, establishing this value as the operational limit for the beam lift design.

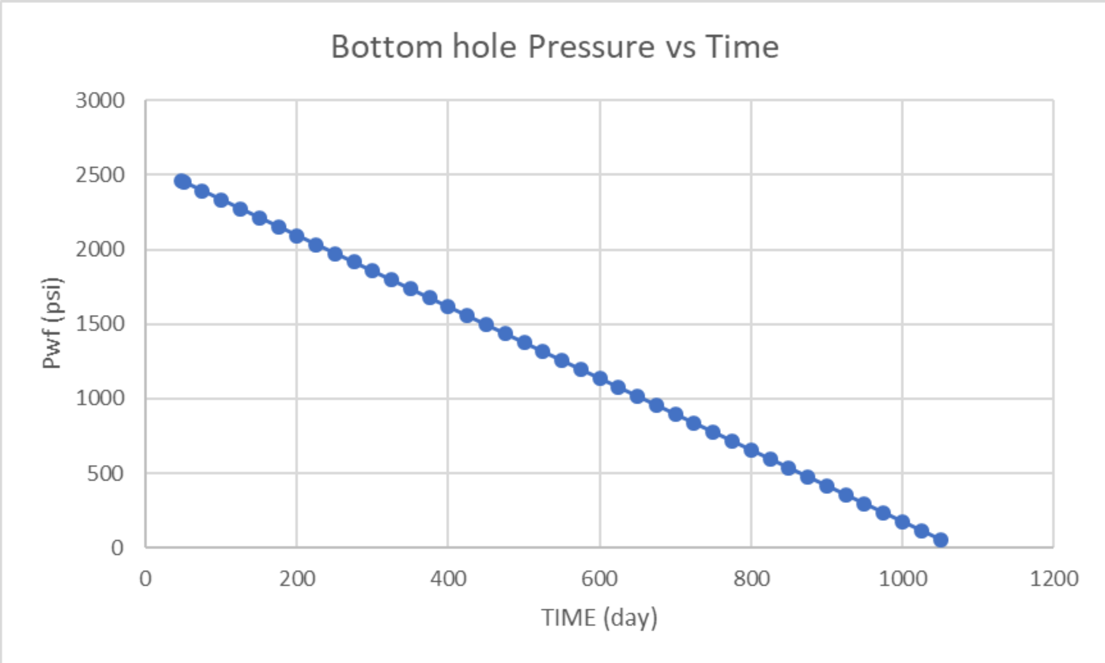


**Figure 4 – Bottom hole pressure plot**

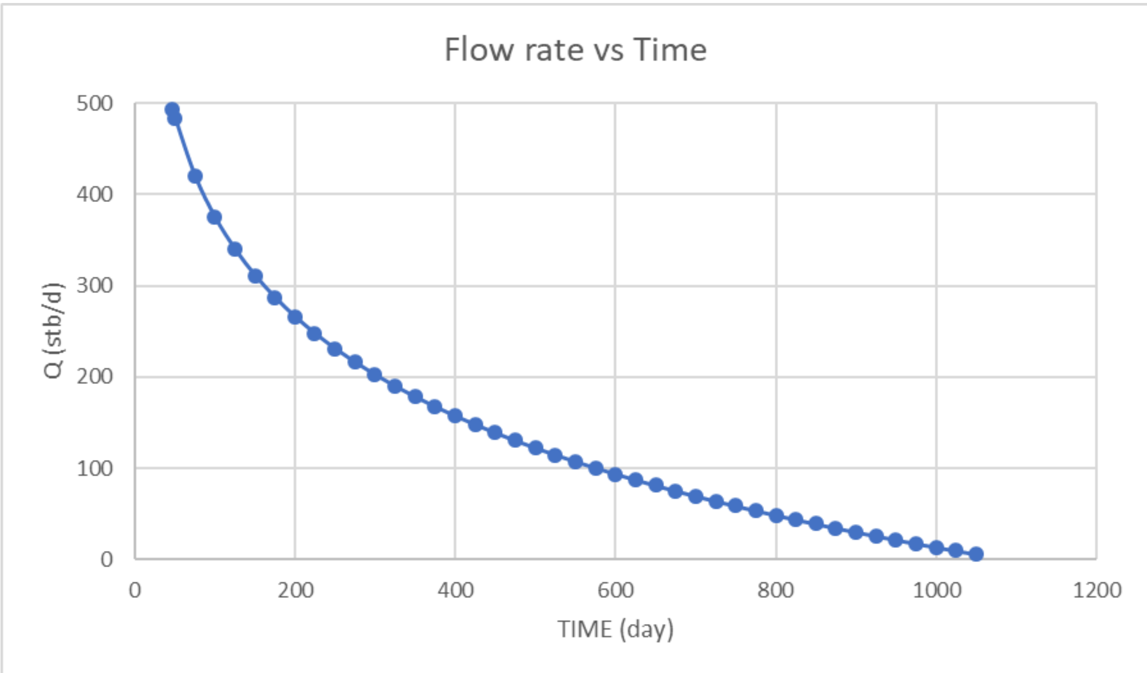


**Figure 5 – Flow rate plot**

The graph above indicates a rapid decline in flow rate, suggesting that designing the beam lift (BL) system for a moderate average flow rate may be more advantageous. Given that the initial investment for the beam lift system is significant, utilizing the QROD program will help determine the optimal design flow rate. When the well production drops below this threshold, the pump can be adjusted to reduce speed and maintain the desired flow rate. Initially, the design will not incorporate the largest pump available to maximize immediate production as oil enters the well. This strategy promotes accumulation within the well, which is beneficial for future production, particularly when bottom hole pressure decreases significantly.

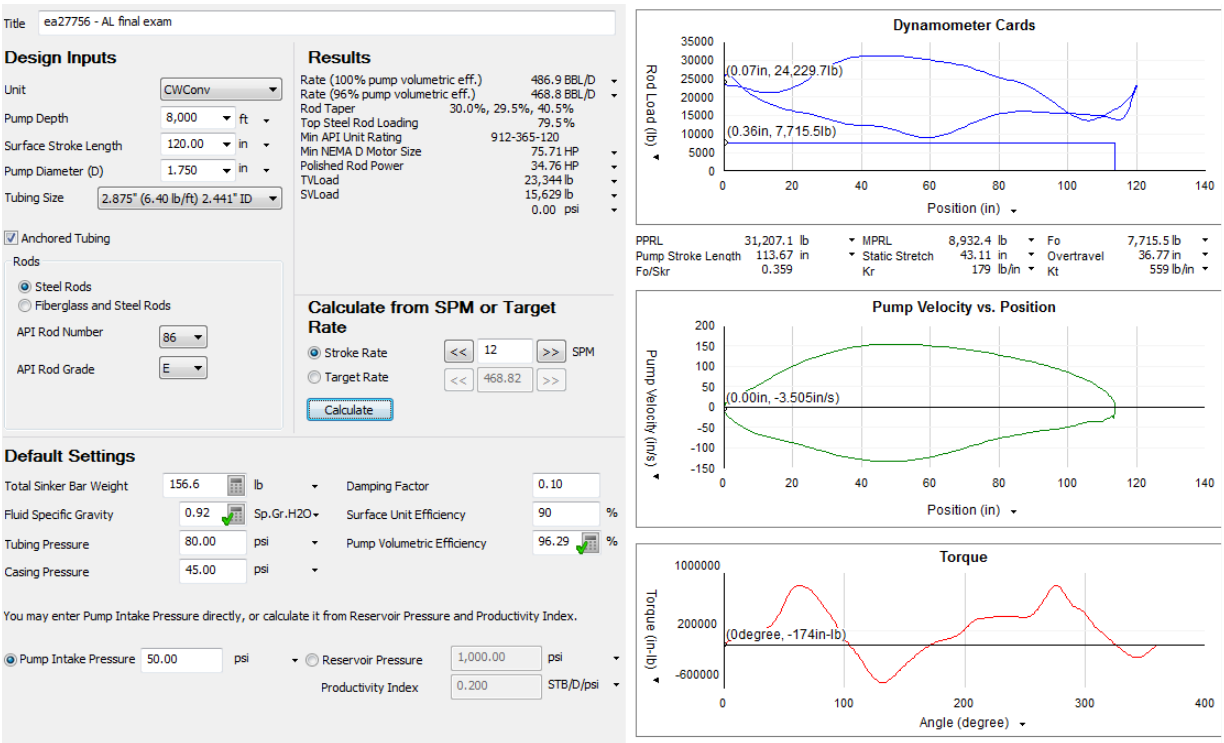


**Figure 6 – QRod software output**

The initial parameters for the beam lift system are established with the understanding that the pump will be gradually slowed down early in the production phase. Consequently, operating at 12 strokes per minute (SPM) will not pose significant issues for the pump.

Another critical consideration is that when the pump is reduced to a very slow speed of 2 SPM, the resulting flow rate will be approximately 47 barrels per day (bpd). This implies that, even when the reservoir is producing at 5 bpd, the overall output will consist of 5 barrels plus the accumulated volume in the well. Although it is unlikely that the beam lift design alone will facilitate the extraction of all available oil from this well, prioritizing higher initial production rates is preferable to achieving lower output later in the well's life cycle.

### 2.2.1. Beam Lift Rod Design

For the conventional pump design, the following parameters have been established: the surface stroke length is set at 120 inches, and the pump diameter measures 1.75 inches. Anchored tubing is preferred for this application, and one sinker bar is utilized. The top steel rod loading is calculated to be 79.5%, which falls within safe operational limits. API 86E [13] rods are selected for use in this system. The following section provides a detailed examination of the rod design.

**Table 3 – Length of the rods (from QRod)**

| | 1" | 7/8" | 3/4" | sinker bar |
|---|---|---|---|---|
| **percentage** | 30 | 29,5 | 40,5 | 0,4 |
| **length** | 2400 | 2360 | 3215 | 25 |
| **wr** | 2,904 | 2,224 | 1,634 | |

Our string is in the oil-water mixture, so we need to calculate buoyancy factor for oil.

38 API= 141.5/SG-131.5 = SG of oil (ɣoil) = 0.8348

Average specific gravity of the mixtu

ɣmix = (0.8348+1.02)/2 = 0.9274

BF = 1-0.127*ɣmix = 0.882

Fo = Ap*L*(0.433)* ɣoil

Ap= π*[(1.75 /2)^2] = 0.243

Fo = 2.405*7000*(0.433)* 0.9274=7727 lbf

α=(S*N2)/70,542 = (120*10^2)/70,542 = 0.24496

### For 3/4” rod – 3215 ft

During downstroke, Wmin = Wrf – Wd

Wrf = (3215ft * 1.634 lbf/ft)*(1-0.127*0.9274) = 4772 lbf

Wd = Wr * L * α = 3215ft * 1.634 lbf/ft * 0.244 = 1287 lbf

σmin= Wmin/cross-section area = (4772-1287)/(π*(0.750/2)^2) = 7890 psi

during the upstroke, Wmax = Wrf + Wd + Fo

σmax= Wmax/cross-section area = (4772+1287+7727)/(π*(0.75/2)^2) = 31206 psi

Smin = σmin / Tmin = 7,890 / 140,000 = 0.056

Smax = σmax / Tmin = 31,206 / 140,000 = 0.222

Smax = 0.805*Smin + Sf => 0.222 = 0.805(0.056) + Sf => Sf = 0.177

Nf = 0.25* (Sf)^(-2.417) = 0.25*(0.177)^(-2.417) = 16.3

Nt = (Nf*10^6)/(N*60*24)= (6.3 *10^6)/(12*60*24) = 943 days = Roughly 2.58 years

### For 7/8” rod – 2360 ft

During downstroke, Wmin = Wrf – Wd

Wrf = (2360ft*2.224lbf/ft + 3215ft * 1.634 lbf/ft)*(1-0.127*0.9274) = 9,403 lbf

Wd = Wr * L * α = 2360ft * 2.224 lbf/ft * 0.244 = 1,285 lbf

σmin= Wmin/cross-section area = (9403-1285-1287)/(π*(0.875/2)^2) = 11,359 psi

during the upstroke, Wmax = Wrf + Wd + Fo

σmax= Wmax/cross-section area = (9403+1285+1287+7727)/(π*(0.875/2)^2) = 32,765 psi

Smin = σmin / Tmin = 11,359 / 140,000 = 0.081

Smax = σmax / Tmin = 32,765 / 140,000 = 0.234

Smax = 0.805*Smin + Sf => 0.234 = 0.805(0.081) + Sf => Sf = 0.168

Nf = 0.25* (Sf)^(-2.417) = 0.25*(0.168)^(-2.417) = 18.44

Nt = (Nf*10^6)/(N*60*24)= (18.44 *10^6)/(12*60*24) = 1,067 days = Roughly 2.92 years

### For 1” rod – 2400 ft

During downstroke, Wmin = Wrf – Wd

Wrf = (2400ft*2.904lbf/ft+2360ft*2.224lbf/ft+3215ft*1.634lbf/ft)*(1-0.127*0.9274) =15,551 lbf

Wd = Wr * L * α = 2400ft * 2.904 lbf/ft * 0.244 = 1,707 lbf

σmin= Wmin/cross-section area = (15551-17707-1285-1287)/(π*(1/2)^2) = 14,351 psi

during the upstroke, Wmax = Wrf + Wd + Fo

σmax= Wmax/cross-section area=(15551+17707+1285+1287+7727)/(π*(1/2)^2)=35,088 psi

Smin = σmin / Tmin = 14,351 / 140,000 = 0.102

Smax = σmax / Tmin = 35,088 / 140,000 = 0.25

Smax = 0.805*Smin + Sf => 0.234 = 0.805(0.081) + Sf => Sf = 0.168

Nf = 0.25* (Sf)^(-2.417) = 0.25*(0.168)^(-2.417) = 18.6

Nt = (Nf*10^6)/(N*60*24) = (18.6 *10^6)/(12*60*24) = 1,076 days = Roughly 2.92 years

| | 1" | 7/8" | 3/4" | sinker bar |
|---|---|---|---|---|
| **percentage** | 30 | 29,5 | 40,5 | 0,4 |
| **length** | 2400 | 2360 | 3215 | 25 |
| **wr** | 2,904 | 2,224 | 1,634 | |
| **wr*L** | 6969,6 | 5248,64 | 5253,31 | 156,55 |
| **wrf** | 15551,85666 | 9403,138 | 4772,685 | 138,11149 |
| **area** | 0,785398163 | 0,60132 | 0,441786 | |
| **wd** | 1707,276346 | 1285,709 | 1286,853 | |
| **sigma-min** | 14351,97897 | 11359,29 | 7890,309 | |
| **sigma-max** | 35088,86553 | 32765,78 | 31206,42 | |
| **Smin** | 0,102514136 | 0,081138 | 0,056359 | |
| **Smax** | 0,250634754 | 0,234041 | 0,222903 | |
| **Sf** | 0,168110875 | 0,168725 | 0,177534 | |
| **Nf** | 18,60693932 | 18,44357 | 16,30903 | |
| **Nt** | 1076,79047 | 1067,336 | 943,8098 | days |
| | 2,950110876 | 2,924209 | 2,58578 | years |

In summary, the weakest rod, measuring ¾ inches in diameter, is projected to fail after approximately 2.5 years if the pump operates continuously at 12 strokes per minute (SPM). However, as previously noted, the beam lift system will be slowed down significantly earlier than this time frame, which is expected to extend the lifespan of the rods beyond the initial calculations. The table above summarizes the key aspects of the rod design.

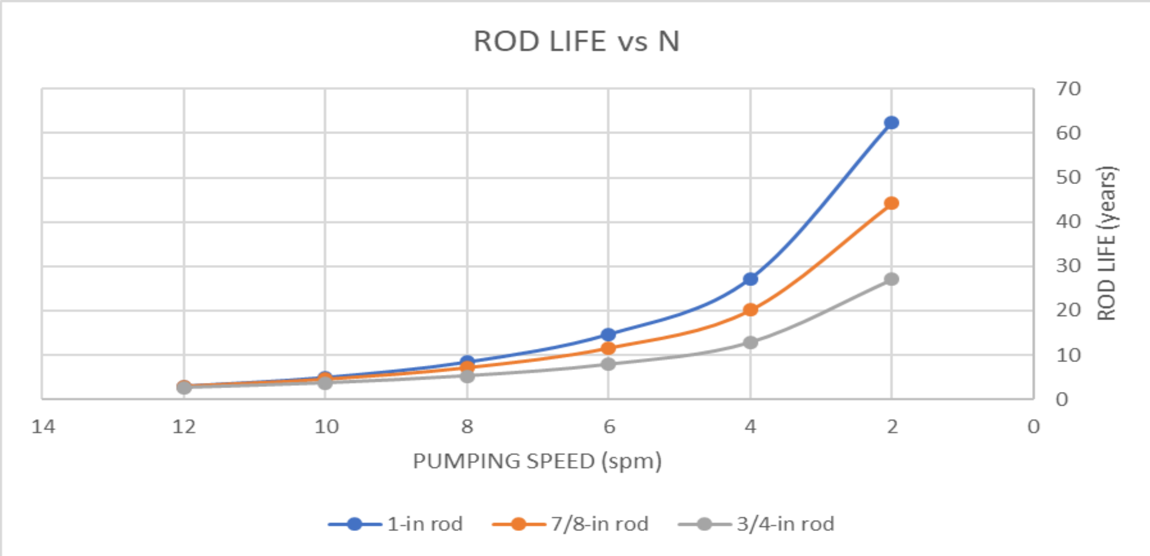


**Figure 7 – Rod life respect to pumping speed**

Figure 7 illustrates the impact of pumping speed on rod life. Utilizing the Utilities package in the Excel file, calculations can be performed to determine the viscosity and frictional losses encountered in the vertical section of the well.

***INPUT DATA***

| RESET | *Fluid Data* | |
|---|---|---|
| Oil Gravity | 38 | API |
| Gas Gravity | 0,7 | |
| Water Gravity | 1,02 | |
| Gas/Liquid Ratio | 200 | Scf/STB |
| Water/Oil Ratio | 1 | bbl/bbl |
| | *Reservoir Conditions* | |
| Pressure | 493 | psi |
| Temperature | 170 | F |
| Pressure Increments | 100 | psi |
| | *Separator Conditions* | |
| Separator Temperature | 100 | F |
| Separator Pressure | 65 | psi |

Calculate Oil Properties

| *Properties At Bubble Point* | | |
|---|---|---|
| Bubble Point Pressure | 1909,46 | psi |
| Liquid Density | 53,0894 | lbm/ft3 |
| Liquid Viscosity | 0,52051 | cp |
| Bo | 1,25187 | Bbl/STB |
| Rs | 400 | Scf/bbl |

**Figure 8 – Viscosity Calculation**

***INPUT DATA***

| RESET | *Fluid Data* | |
|---|---|---|
| Density | 60,7 | lbm/ft3 |
| Viscosity | 0,52 | cp |
| | *Wellbore Data* | |
| Diameter | 2,441 | in |
| Length | 8000 | ft |
| Angle | 0 | deg |
| Roughness | 0,0006 | |
| | *Flow Data* | |
| Pressure Drop | | psi |
| Flowrate | 493 | Bbl/D |

Calculate Pressure Drop

**Pressure Drop =** 6,1 psi

Calculate Flow rate

**Figure 9 – Friction Pressure Drop Calculation**

At this point, the system efficiency can be evaluated using the following formulas:

$$e_s = \frac{HHP}{P_{pm}}$$

$$HHP = \frac{q(p_{disch})}{58{,}771}$$

$HHP =$ hydraulic horse power

$q =$ flow rate (Bbl/day)

$p_{disch} =$ pump discharge pressure (psi)

$p_{fric} =$ pipe friction (psi)

$p_T =$ pressure needed to exit the well (psi)

$p_{wf} =$ flowing pressure at the bottom (psi)

$$p_{disch} = 0.433\gamma_f(TVD) + p_{fric} + p_T - p_{wf}$$

### 2.3. Electric Submersible Pump (ESP) Design

For the electric submersible pump (ESP) design, it is essential to select a pump from the catalog capable of accommodating the required flow rate. Before commencing calculations, it is important to consider the advantages and disadvantages of ESP pumps. These pumps are particularly beneficial in scenarios involving high flow rates, deviated wells, and small locations. However, there are notable drawbacks, such as reduced efficiency due to gas interference, high initial costs for purchase or repair, and elevated electricity expenses. Therefore, it becomes evident that the application of ESP pumps may not be ideal for this unconventional reservoir, especially considering the absence of high flow rates; thus, the smallest ESP pumps may be the most appropriate choice for this reservoir.

On day 47, the recorded flow rate was 493 STB/day. Based on this value, the 400-180 pump from the catalog is suitable for selection.

Background calculations:
Flow rate (q) = 493 STB/day

Mixed specific gravity (γ_mix) = 1.02(0.5) + 0.8348(0.5) = 0.9274

Mixed viscosity (μ_mix) = 0.52 cp (from the oil properties spreadsheet)

Frictional pressure drop (Δp_fric) = 6 psi (from the incompressible fluid spreadsheet)

This selected pump provides a head of 18.3 ft per stage and an optimal flow rate of 216 STB/d.

Performance Summary

| Best Efficiency Data - 60Hz | | | | |
|---|---|---|---|---|
| Optimum Flow Rate [BPD] | Operating range [BPD] | Head per Stage [ft] | Power per Stage (HP) | Efficiency [%] |
| 216 | 75-300 | 18.3 | 0.07 | 41 |

| Best Efficiency Data - 50Hz | | | | |
|---|---|---|---|---|
| Optimum Flow Rate [M³/D] | Operating range [M³/D] | Head per Stage [m] | Power per Stage (kW) | Efficiency [%] |
| 29 | 10-40 | 3.8 | 0.03 | 41 |

**Figure 10 – Pump 400-180 Performance Summary [14]**

The net pressure for the pump, at T = 47 days, can be calculated as follows:

$\Delta p$ = 8000 (0.433)(0.9274) + 100 + 6 − 2462 = 856 psi

Δp=8000(0.433)(0.9274)+100+6−2462=856psi

The pressure drop per stage ($\Delta ps$) is given by;

$\Delta ps$=(18.3)(0.433)(0.9274) = 7.3486 psi/stage

The number of stages required can be determined using:

Number of stages = (856) / (7.3486) ≈ 117 stages

To calculate the horsepower required, the following formula is applied:

Horsepower =1.7×10−5×493×7.3486≈0.0615 hp/stage

Thus, the total horsepower needed is:

Total horsepower = (0.0615 hp/stage) ×117 stages ≈ 7.2 HP

Consequently, a 10 HP motor is selected from the catalog to meet the requirements.

| 60Hz | | | | | | | 50Hz | | | | | | |
|---|---|---|---|---|---|---|---|---|---|---|---|---|---|
| HP | kW | Volts | Amps | Type | Length [ft] | Weight [lb] | HP | kW | Volts | Amps | Type | Length [m] | Weight [kg] |
| 10 | 7.5 | 436 | 15 | S | 5.1 | 240 | 8.3 | 6.2 | 363 | 15 | S | 1.55 | 109.0 |
| | | | | UT | 4.9 | 200 | | | | | UT | 1.49 | 90.7 |

**Figure 11 – Motor Selection Chart [14]**

**when T=500 days,**

$$\Delta p = 8000(0.433)(0.9274) + 100 + 6 - 1375 = 1943 \text{ psi}$$

Number of stages = 1943/7.3486 = 265 stages.

Horsepower = 1.7 x 10-5 x 122 x 7.3486 = 0.015 hp/stage

Total horsepower = 0.015 hp/stage * 265 stages = 4 HP

**when T=850 days,**

$$\Delta p = 8000(0.433)(0.9274) + 100 + 6 - 535 = 2788 \text{ psi}$$

Number of stages = 2788/7.3486 = 379 stages.

Horsepower = 1.7 x 10-5 x 39 x 7.3486 = 0.0048 hp/stage

Total horsepower = 0.0048 hp/stage * 379 stages = 1.85 HP

**Table 5 – ESP Design Summary**

| T, days | Q, stb/day | net pressure | | power | # of stages |
|---|---|---|---|---|---|
| 47 | 493 | 2462 | 0.11 | 7,20 | 117 |
| 500 | 122 | 1375 | 0.37 | 4,00 | 265 |
| 850 | 39 | 535 | 0.11 | 1,85 | 379 |

The pump model 400-180 has a limit on the number of stages, which is capped at 341. This limitation presents an additional constraint for the design of the ESP system.

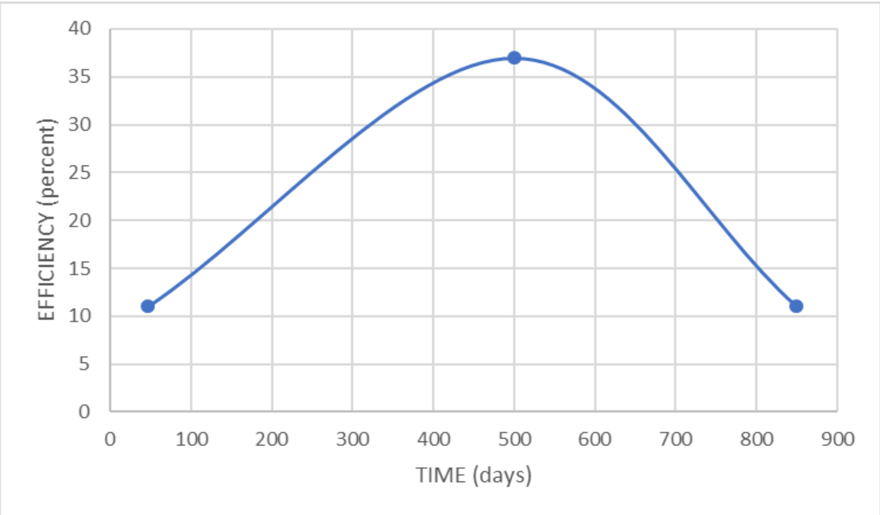


**Figure 12 – ESP Pump Efficiency Chart**

Upon examining the efficiency chart, it is evident that high efficiency is not achieved during the initial high flow rate phase, which occurs shortly after the 47-day mark in production.

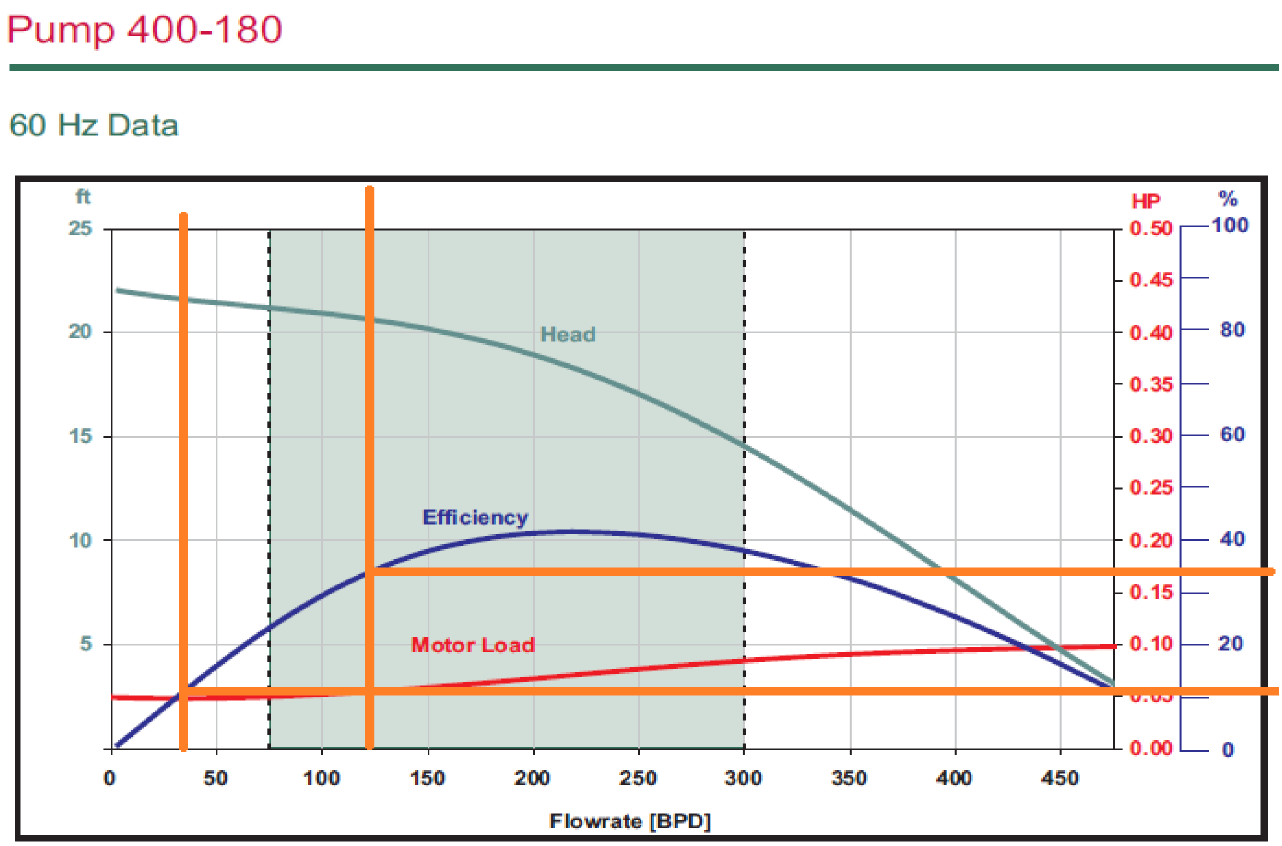


**Figure 13 – ESP 400-180 Pump Hz Data [14]**

The chart above, Figure 13, was utilized for the efficiency calculations. With the gas lift system, production is not sustained when the bottom hole pressure (Pwf) falls below 535 psi. In contrast, the beam lift system allows for oil production until Pwf reaches 452 psi. The use of an ESP pump is not recommended for this type of unconventional reservoir.

## Conclusion

In conclusion, the evaluation of artificial lift systems for the unconventional reservoir under consideration highlights the distinct operational thresholds and efficiency limitations of each method. The gas lift system demonstrates a minimum bottom hole pressure requirement of 535 psi for sustained production, while the beam lift system maintains production capabilities down to a pressure of 452 psi. Given these findings, the beam lift system emerges as the more viable option for this well, particularly considering its ability to produce at lower pressures and its relative cost-effectiveness in the context of the reservoir's characteristics.

The study emphasizes the importance of selecting an appropriate artificial lift method tailored to the specific conditions of the reservoir, ensuring optimal production rates and extending the economic life of the well. Future work should focus on monitoring and adjusting the chosen system in response to ongoing reservoir depletion, as well as exploring potential enhancements to improve efficiency and adaptability in unconventional reservoirs. Overall, this analysis provides valuable insights into the effective management of hydrocarbon production through the strategic application of artificial lift technologies.

## References

1. Alagoz E, Dündar EC. (2024) A Comparative Analysis of Production Forecast for Vertical Gas Wells: Fractured vs. Non-Fractured. International Journal of Earth Sciences Knowledge and Applications 6: 194-202. https://doi.org/10.23880/ppej-16000371.
2. Alagoz E, Dündar EC (2024) A Comparative Analysis of Production Forecast for Vertical Gas Wells: Fractured vs. Non-Fractured. International Journal of Earth Sciences Knowledge and Applications, 6: 194-202. https://www.ijeska.com/index.php/ijeska/article/view/403
3. Laalam A, Khalifa H, Ouadi H, Keltoum Benabid M, Stanley Tomomewo O, et al. (2024) Evaluation of

empirical correlations and time series models for the prediction and forecast of unconventional wells production in Wolfcamp A formation. In Unconventional Resources Technology Conference 2883-2910. Unconventional Resources Technology Conference (URTeC). https://doi.org/10.15530/urtec-2024-4043738.

4. Dehdouh A, Bettir N, Khalifa H, Kareb A, Al Krmagi, M (2024) Optimizing Recovery in Unconventional Reservoirs by Advancing Fishbone Drilling Technology in the Bakken Formation, Williston Basin. In ARMA US Rock Mechanics/Geomechanics Symposium ARMA. https://doi.org/10.56952/ARMA-2024-0919.
5. Al Krmagi M (2024) Environmental Impacts and Treatment Technologies in Hydraulic Fracturing Water Management. International Journal of Earth Sciences Knowledge and Applications 6: 262-267. https://www.ijeska.com/index.php/ijeska/article/view/410.
6. Al Krmagi M (2024) Environmental Impacts and Treatment Technologies in Hydraulic Fracturing Water Management. International Journal of Earth Sciences Knowledge and Applications 6: 262-267. https://doi.org/10.23880/ppej-16000380.
7. Alagoz E, Sharma MM (2021) Investigating shale-fluid interactions and its effect on proppant embedment using NMR techniques. In ARMA US Rock Mechanics/Geomechanics Symposium ARMA. https://onepetro.org/ARMAUSRMS/proceedings-abstract/ARMA21/All-ARMA21/ARMA-2021-1129/467923.
8. Alpkiray M, Dundar EC (2023) A Glance on Hydraulic Fracturing: Benefits, Concerns, and Future. Science Journal of Energy Engineering 11: 19-25. https://doi.org/10.11648/j.sjee.20231102.11.
9. Alagoz E, Wang H, Russell RT, Sharma MM (2020) New experimental methods to study proppant embedment in shales. In ARMA US Rock Mechanics/Geomechanics Symposium ARMA. https://doi.org/10.1007/s00603-021-02646-1.
10. Alagoz E, Dundar EC, Al Krmagi M (2024) Numerical Simulator of Production Forecast for Multi-Lateral Oil Well using MATLAB-based Simulator. Progresses in Petrochemical Science, Crimson Publishers. https://crimsonpublishers.com/pps/pdf/PPS.000643.pdf.
11. Alagoz E, Dundar EC (2024) Forecasting Gas Well Production and Analyzing Pressure Dynamics: A Study of Transient Flow and Pressure Drop in Natural Gas Formation. Environ Sci 2: 000115. https://doi.org/10.23880/jeesc-16000115
12. Alagoz E, Dundar EC, Al Krmagi M (2024) Numerical Simulation of a Multilateral Saturated Reservoir using MATLAB-based Simulator. Petroleum and Petrochemical Engineering Journal, Medwin Publishers.